# Heavy Metal and Radionuclide Contaminant Migration in the Vicinity of Thermal Power Plants: Monitoring, Remediation, and Utilization

**Debashish Sengupta and Sudha Agrahari**

**Abstract** Environmental pollution has been an important issue particularly in a period which is witnessing a rapid industrial growth. The major sources of heavy metal and radionuclide pollution in urban areas are anthropogenic which includes the fossil, coal combustion, etc. Coal, one of the most abundantly found materials in nature, has trace quantities of primordial radionuclides, $^{238}$U, $^{232}$Th, and $^{40}$K. Thus, combustion of coals in thermal power plants (TPPs) is one of the major sources of environmental pollution enhancing the natural radiation in the vicinity of TPPs. Fly ash, the main residue from the combustion of pulverized bituminous or sub-bituminous coal (lignite), is directly disposed of in large ponds in the nearby areas of TPPs. This problem is of particular significance in India, which utilizes coals of very high ash content (approximately 40–55 %). Background knowledge, i.e., monitoring of the origin, chemistry, and risks of toxic heavy metals (Pb, Cr, As, Zn, Cd, Cu, Hg, and Ni) and radionuclides in contaminated soils, is necessary for the selection of appropriate remedial options. For this purpose, soil, ash, and coal samples were collected from the nearly areas of TPPs. In order to validate the fact of heavy metal and radionuclide contaminant migration in the vicinity of TPPs, several geophysical, radiochemical, and trace element analysis tests were carried out. Lack of proper insulation at the bottom of the ash disposal ponds enhances the chances of groundwater contamination. The direct current (dc) resistivity survey, employing Schlumberger configuration, was undertaken to identify the local subsurface and to estimate the depth of contamination around ash ponds near a thermal power plant in Eastern India. A continuous conductive zone with resistivity <5 Ωm was identified throughout the studied region at a depth of about 2–10 m indicating the presence of water with higher ionic concentration. The study was also supported by the radiometric geophysical measurements indicating the presence of radionuclides in the vicinity of ash ponds. Groundwater samples have also been collected

D. Sengupta (✉) · S. Agrahari
Department of Geology and Geophysics, Indian Institute of Technology Kharagpur, Kharagpur, India
e-mail: dsgg@gg.iitkgp.ernet.in; dsgiitkgp@gmail.com

S. Agrahari
e-mail: sudha@gg.iitkgp.ernet.in

© Springer Science+Business Media Singapore 2017

D. Sengupta and S. Agrahari (eds.), *Modelling Trends in Solid and Hazardous Waste Management*, DOI 10.1007/978-981-10-2410-8_2

from the tube wells located near the ash ponds and analyzed for pH, TDS and trace elements. Results of the chemical analysis show high values of TDS and high concentration of the toxics. The studies on the geochemistry of the ash ponds have shown that the ashes are characterized by high concentration of As, Pb, Cu, Ni, Fe, Zn, Cr, Co, and Mn all of which exceeded the crustal abundance by a factor of 3–5. The high concentration of the toxics (As, Al, Li, Zn, Ag, Sb, Si, Mo, Ba, Rb, Se, Pb) in the water samples implies significant input from the ash pile due to leaching. This increases the TDS values of the water. Radiochemical characterization of coal, ash, and soil samples was done based on Radium equivalent activity, dose rate, and hazard index. The activity concentration variations infer to the high radioactivity in the vicinity of the ash ponds up to a radius of 500 m and indicate a decreasing trend beyond 500 m. In general, the radioactivity of the nearby area showed three to four times higher values than the prescribed limit, and the hazard index was estimated as unity. In order to mitigate the associated risks, make the land resource available for agricultural production, enhance food security, and scale down land tenure problems, remediation of contaminated soil is necessary. Immobilization, soil washing, and phytoremediation are one of the best technologies for cleaning up of contaminated soils but have been mostly demonstrated in developed countries. Such technologies need high recommendation for field applicability and commercialization in the countries (developing) where agriculture, urbanization, and industrialization are causing environmental degradation. The utilization of contaminated soil is also discussed. Rare earth elements, heavy metal, and radionuclides, which are of economical importance, can be extracted from the contaminated soil and the remainder can be utilized in filling voids and reclamation of the mining lands.

**Keywords** Thermal power plants · Radionuclides · VES · Radon exhalation

## Introduction

One of the most significant fuel sources for steam and energy production is coal. Coal combustion in thermal power plants increases the three aspects of atmospheric pollution. Huge quantities of gaseous and particulate pollutants ($SO_2$, $NO_x$, $CO_2$, hydrocarbons, and fly ash) are discharged into the local environment. Additionally, small amounts of toxic trace elements (As, Hg, and Cd) and minute amounts of radionuclides (U, Th, and their radioactive daughters) are also released, which may have a radiological impact on the environment.

Coal is serving as a major power source in our country by fulfilling the 70 % electricity demand. Remaining part of power generation comes from the hydroelectricity and nuclear power plants. Coal ash is the residual after coal combustion, which was not fully burnt. The volume of the end residue generated after coal combustion is dependent on the quality of coal used in thermal power stations. In Indian thermal power stations, bituminous or sub-bituminous type of coal is used which is generating about 55–60 % ash content. Consequently, 160 million tons of

ash is produced yearly and is projected to reach 300 million tons per annum by 2016–2017 (Singh et al. 2011). Because of the enrichment of radionuclides in coal ash, the management of coal ash is a major environmental problem.

Fly ash and bottom ash are mainly two types of solid wastes, which are generated as a byproduct after coal combustion. Trace elements, which are smaller in size and larger in surface area, got absorbed on the ash particles (Culec et al. 2001). Bottom ash is the coarse-grained fraction of ash, which precipitates due to its weight and settles at the bottom of the furnace. This course-grained fraction is directly thrown into the closer ash ponds. Due to the light weight of fly ash particles, it spreads and distributes in the vicinity by air, henceforth deposits on the soil surface, which increases the radioactivity level of the local environment.

The toxicity of the soil and groundwater gets enhanced due to continuous disposal of bottom ash into the ash ponds. The solid wastes generated after coal combustion are released either directly through the stack releases or indirectly from waste storage areas. Most of the power stations in India operate close to coal fields, which are mainly located in the eastern region of India, i.e., Bihar, Jharkhand, and West Bengal. Due to dense population density in these areas, the environmental aspect is of major concern. According to Lalit et al. (1986), the radioactivity level of coals from these coal fields is on the higher side compared to the other coal fields. Consequently, population residing in this particular region is facing more environmental hazard.

Out of 31 coal-based thermal power plants of eastern India, 14 of these are located in West Bengal. Kolaghat, Durgapur, and Bandel are one of the biggest thermal power plants of eastern India with a capacity of 1260, 350, and 530 MW of electricity, respectively. The Kolaghat thermal power plant is located in Midnapur district, West Bengal (22°27′–22°25′ N latitude and 87°50′–87°55′ E longitude). Coal used in this thermal power plant is of bituminous type and 1260 MW power is generated in six units of 210 MW. The Durgapur thermal power plant is situated in Burdwan district, West Bengal (22°56′–23°53′ N latitude and 86°48′–88°25′ E longitude), and Bandel thermal power plant in Hooghly district, West Bengal (23° 39′32′′–23°01′20′′ N latitude and 87°30′15′′–88°30′20′′ E longitude). Due to the use of low-grade coal (sub-bituminous), huge amount of ash is produced, which is thrown away in ash ponds. These ash ponds are open and exposed to the sun, and therefore the slurry starts drying and becomes hard and compact, which later becomes a source of radiation hazard.

Recently, the use of fly ash is increased many folds as building material in the form of ash bricks and as filling material for underground cavities. Thus it is evident to monitor the radiation risk to the population.

Here, we are going to discuss the three power plants (Bandel, Durgapur, and Kolaghat) in detail. For this purpose, these power plants were investigated (Mandal and Sengupta 2006; Maharana et al. 2010; Mondal et al. 2006; Parial et al. 2015, 2016). The general objectives were as follows:

i. The determination of the presence of radionuclides (U, Th, and K) in coal and ash, and their enrichments in ash after coal combustion. It gives an idea about the environmental hazard of the area.
ii. Because of the improper management of ash, it is directly dumped into the open ash ponds and thereby severely affecting the surrounding population. Therefore, the radiological impact is determined by computation of the dose rate.
iii. The determination of the subsurface contamination was done using noninvasive geophysical methods.
iv. A comparison between the radiometric data in the vicinity of Kolaghat, Durgapur, and Bandel thermal power plants is required in order to estimate the radiation potential in these areas.
v. Hazard index estimation for the fly ash admixture for cement, concrete, and fly ash bricks.

## Materials and Methods

Characterization of the nearby areas of thermal power plants, in terms of heavy metals and radionuclide contaminant migration, is done by conducting field-based and lab-based analyses. Mostly field-based studies include noninvasive methods; however, lab-based analyses are done by conducting several geochemical tests. In this section, a brief summary of all the methods utilized is presented, which are used for the characterization of the vicinity of the TPPs.

1. ***Noninvasive Geophysical investigations:***

   i. ***In situ radiometric study***
   A reconnaissance survey was conducted in and around Kolaghat thermal power plant (KTPP) based on in situ radiometric analysis. The ambient terrestrial dose rate was measured using a handheld scintillation counter. The counter is commonly known as micro-R survey meter. The model used was UR-709, manufactured by Nucleonix Systems Private Limited, Hyderabad, India. Soil samples from high ambient dose rate areas were collected for lab-based radiometric analysis. The locations of the sampling points were marked using GPS (manufactured by Trimble, Juno ST Handheld, Trimble Juno Series).

   ii. ***Subsurface characterization using direct current (dc) resistivity method***
   1D vertical electrical sounding (VES) measurements were conducted using Terra Science resistivity meter. VES were measured at twelve locations around KTPP and at one reference site outside the contaminated area. These twelve soundings were conducted in the vicinity of the two ash ponds and within a radius of 1 km from the ash disposal sites using Schlumberger electrode configuration. To achieve greater depth of penetration, longest

possible profile at every location was selected. The measurements were carried out during winter and spring season to avoid the interferences due to rain. In dc resistivity sounding, current ($I$) is injected into ground through a pair of electrodes and the potential difference ($\Delta V$) is measured by another pair of electrodes (potential electrodes). The placement of these two pairs of electrodes determines the array configuration. According to the Ohm's law, the ratio of the potential difference to the current injected estimates the resistance. The apparent resistivity is estimated using Ohm's law (Eq. 1):

$$\rho_a = G.\left(\frac{\Delta V}{I}\right) \tag{1}$$

where $G$ is the geometric factor due to the array configuration, $\Delta V$ is the potential difference between the two potential electrodes, and $I$ is the current injected. A detailed discussion can be found in Telford et al. (1990). The greater the current electrode separation, the greater is the depth of penetration.

2. ***Laboratory (Geochemical) investigations***

   i. ***Sample collection and preparation***
   The feed coal samples were collected from inside of the power plants. The coals from four different coal fields (Jharia, Talchir, Giridih, and Raniganj) of lower Gondwana age were mixed together and pulverized before combustion. The entire mass of generated ash in the power plants was disposed off in large ponds located near the power plant. Ash samples were collected from the ash ponds. Soil samples were collected from the villages in the vicinity of the active ash ponds. The collected samples were stored in polyethylene bags. The samples were homogenized and then dried for 24 h in an air circulation oven at 110 °C. About 100 g of the dried samples were weighed and sealed in gas-tight, radon impermeable, cylindrical polyethylene containers (7.0 cm height and 6.5 cm diameter). These samples were then left for 15 days in order to allow for radium, thorium, and their short-lived progenies to reach secular equilibrium before radioactive determination of uranium and thorium. Subsequently, gamma-ray spectrometric analyses of the samples were conducted for the estimation of the $^{238}$U, $^{232}$Th, and $^{40}$K in soil, coal, and ash samples. The analysis was performed at the Radiochemistry Division, Variable Energy Cyclotron Centre, BARC, Kolkata.

   ii. ***Radioactivity measurements***
   Low-level gamma-ray spectrometry was used to determine the activity concentrations of $^{226}$Ra, $^{232}$Th, and $^{40}$K in fly ash samples. The present system is an intrinsic p-type coaxial HPGe detector with a relative efficiency of 50 % and energy resolution of 1.9 keV at 1332.5 keV for $^{60}$Co. It is placed vertically in a lead cylindrical shield of 12 cm thickness and 65 cm height to reduce the background radiation. A low ambient temperature is

maintained by electric refrigeration system. A solid radionuclide mixture of gamma reference materials, sealed in standard cylindrical polyethylene containers (7.0 cm in height and 6.5 cm diameter), was used to estimate the absolute efficiency of the gamma-ray spectrometer.

a. *Estimation of Radiation dose and Hazard index*
Natural radioactivity is a consequence of the radioactive emission of mainly $^{238}$U, $^{232}$Th, and $^{40}$K. Potassium can be measured with the help of its own peak (1460 keV); however, uranium and thorium are measured with the help of their daughter products. For uranium the peaks 295 keV, 352 keV ($^{214}$Pb), and 609 keV ($^{214}$Bi), and for thorium the peaks of 338 keV, 911 keV ($^{228}$Ac), 239 keV ($^{212}$Pb), 727 keV ($^{212}$Bi), and 583 keV ($^{208}$Tl) are considered (Abd El-mageed et al. 2011; Khan et al. 2002). Efficiency of these respective peaks is calculated using a standard Eu$^{152}$ sample, with known half-life, with the help of Eq. (2). Each sample is measured for 40,000 s to obtain a reasonable ϒ-ray peak area. From this peak area the activity is measured with the help of a multi-channel analyser Canberra DSA 1000, which is connected to computer through Genie 2 K software:

$$\varepsilon = \frac{CPS \times 100}{A_t \times I}, \tag{2}$$

where $\varepsilon$ = Efficiency; $CPS$ = Counts per second; $A_t$ = Activity of $^{152}$Eu; and $I$ = Intensity of $^{152}$Eu.

b. *Absorbed Dose Rate*
It is basically the radiation received by any person per kilogram of its mass. The conversion factor required to calculate absorbed dose rate at 1 m above the ground surface, due to uniform distribution of gamma radiations from $^{238}$U, $^{232}$Th, and $^{40}$K, is calculated by the method proposed by the UNSCEAR 2000. The equation is mentioned below:

$$\mathrm{D\,(nGyh)} = 0.461\mathrm{A_U} + 0.623\mathrm{A_{Th}} + 0.0414\mathrm{A_K}, \tag{3}$$

where $\mathrm{A_U}$, $\mathrm{A_{Th}}$, and $\mathrm{A_K}$ are the specific activities of $^{238}$U, $^{232}$Th, and $^{40}$K in Bq kg$^{-1}$.

c. *Annual Effective Dose Rate*
It basically gives us an idea about the internal and external radiation exposures. It is calculated using the conversion coefficients (0.7 SvGy$^{-1}$) and 0.2 as the outdoor occupancy factor, as proposed by UNSCEAR 2000:

$$\mathrm{AED\,(mSvy^{-1})} = \mathrm{D\,(nGyh^{-1})} \times 8760\,\mathrm{(hy^{-1})} \times 0.2 \times 0.7\mathrm{Sv\,Gy^{-1}} \times 10^{-6}. \tag{4}$$

d. *Radium Equivalent*
It describes the gamma output from different mixtures of U, Th, and K in samples and helps in comparison of radiation exposure due to different radioisotopes:

$$Ra_{eq} = A_U + 1.43\ A_{Th} + 0.077\, A_K. \quad (5)$$

The equation is proposed by UNSCEAR 2000, based on the assumption that contributions from other radionuclides are insignificant.

e. *Hazard Index*
It is the index that indicates the external exposure due to the radioisotopes in the environment:

$$H_{ex} = A_U/370 + A_{Th}/259 + A_K/4810. \quad (6)$$

$H_{ex} < 1$ is considered to be within limit, and $H_{ex} > 1$ is unsafe and equivalent to 370 Bq $kg^{-1}$.

iii. ***Radon exhalation rate measurements***
Radon exhalation measurements were undertaken using Cup dosimeters. The fly ash samples were dried and sieved through a 100-mesh sieve and placed in cups/cans, up to the sensitive volume (diameter 7.0 cm and height 7.5 cm). An LR-115 type-II solid-state nuclear track detector (2 cm × 2 cm) was fixed at the top, within the cup. The sensitive, lower surface of the detector is freely exposed to the emergent radon and was capable of recording the alpha particles, due to the decay of radon in the cup. After a week or more, radon and its daughters attain equilibrium. Thus, the equilibrium activity of emergent radon could be obtained from the geometry of the cup and time of exposure. After exposure for 100 days, the detectors from all the cups were retrieved. For the revelation of tracks, the detectors were etched in 2.5 N NaOH at 60 °C for a period of 90 min, in a constant-temperature water bath. Alpha tracks on the exposed face of the detector foils were scanned using an optical microscope at magnification of 400 times. From the track density, the radon activity was obtained using a calibration factor of 0.056 Tr $cm^{-2}$ $d^{-1}$ obtained from an earlier calibration experiment, for an LR-115 type-II detector (Singh et al. 1997). An experiment was performed in order to study the effect on radon exhalation rates by adding varying amounts of fly ash. The measurement of the exhalation rate of radon from a homogeneous mixture of (i) fly ash and soil and (ii) fly ash and cement was obtained. For this purpose, different percentages of fly ash were introduced in the soil and cement, keeping the total weight of the sample constant. All the samples were dried and sieved through a 100-mesh sieve before mixing, for homogeneity.
The exhalation rate was estimated from the relationship provided by Fleischer and Morgo-campero (1978) and Khan et al. (1992):

$$E_x = \frac{CV\lambda}{A[T + 1/\lambda\{e^{-\lambda T} - 1\}]}, \tag{7}$$

where $E_x$ is the radon exhalation rate (Bq $m^{-2}$ $h^{-1}$), $C$ is the integrated radon exposure measured by an LR-115 type-II plastic track detector (Bq $m^{-3}$ h), $V$ is the effective volume of Can ($m^3$), $\lambda$ is the decay constant for radon ($h^{-1}$), $T$ is the exposure time (h), and $A$ is the area covered by the Can ($m^2$), respectively.

## Results and Discussion

Environmental pollution measurements in and around TPPs were done by adopting two-step methodology. At first, the sites were investigated using noninvasive geophysical measurements and thereafter based on the preliminary noninvasive geophysical survey results, locations were selected for sample collection. As a second-step methodology, geochemical tests of soil/ash samples were conducted in laboratory.

i. ***Noninvasive Geophysical investigation results:***
The isorad map, based on surface gamma radiation, from the vicinity of Kolaghat thermal power plant is shown in Fig. 1. The surface radiation varies from 4.5 to 9.2 μRhr$^{-1}$ showing an increasing trend toward northwest. The maximum surface radiation dose was observed toward the northern edge of the

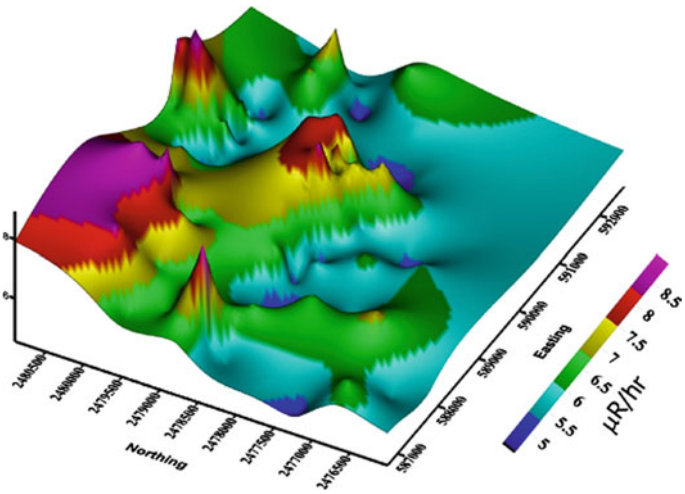



**Fig. 1** Isorad map based on surface radiation in the vicinity of Kolaghat thermal power plant (after Parial 2016)

area, which coincided with the ash ponds present in the area. This indicated the presence of a high background radiation in the vicinity of the thermal power plant as well as the ash ponds (Parial 2016).

These observations emphasize that the contamination is maximum close to the ash ponds. The leachate from the ash ponds consists of water-soluble metallic species, which are posing maximum risk to groundwater. Generally, clay acts as a natural barrier to the leachates; however, due to high porosity sand not only acts as a potential aquifer but also allows an easy passage to the leachates from the waste dumps. Extreme precipitation events during monsoon can allow higher infiltration of the contaminants from the ash dumps to the deeper levels. Therefore, to assess the status of groundwater aquifers noninvasive vertical electrical sounding measurements were conducted in and around the Kolaghat thermal power plant. VES measurements using Terra Science resistivity meter (DDR2) were conducted at 12 locations and at one reference site. The reference site was located ∼3 km northwest of the thermal power plant; five soundings, VES-S4 to VES-S8, were in the vicinity of the two ash ponds; VES-S1 to VES-S3, VES-S9, VES-S10 were located within a radius of 1 km from the ash disposal sites. VES-S11 was located to the east of the thermal power plant, downstream of the River Rupnarayan, and VES-S12 was present south of the thermal power plant within 1 km (Fig. 2). The maximum profile length in the thirteen soundings varied between 100 and 800 m. The maximum profile length measured was at VES-S12 and the reference site.

These investigations help in understanding the subsurface in the region close to the thermal power plant. The 1D interpreted models infer the presence of a thick conductive zone (resistivity < 5 Ωm) throughout the region (Fig. 2). This conductive layer starts at a depth ranging from 2 to 10 m from the top and its thickness ranges between ∼27 and 39 m (Parial et al. 2015). Based on the available borehole data and the earlier observations (Mandal et al. 2007), this zone is identified as saturated clay with high concentration of various ionic species. From the borehole information, the presence of sandy layers at the top facilitates the percolation of the leachate into the deeper clay layer. Although clay is considered as a repository of trace/heavy metals, continuous loading of these species at higher concentration results in enhanced percolation. Ultimately, it percolates up to the deeper aquifer at a depth of ∼50 m (Fig. 2). As groundwater is the major source of potable water in this region, an extension with the previous studies by Mandal et al. (2007), Parial et al. (2015) emphasizes the importance of meticulous monitoring of the groundwater quality and the temporal variation in the nature of the contaminant(s).

ii. ***Geochemical investigation results:***

The geochemical studies of water samples, collected from a 50-m-deep tube well in the vicinity, by Mandal et al. (2007), further strengthened the presence of the mentioned contaminated layer (<5 Ωm). They confirmed the presence of high TDS count (550–760 ppm), abundance of $Ca^{2+}$, $Na^{+}$, presence of anions ($HCO_3^{-}$, $SO_4^{2-}$, and $Cl^{-}$), and high concentration of trace elements (like Li,

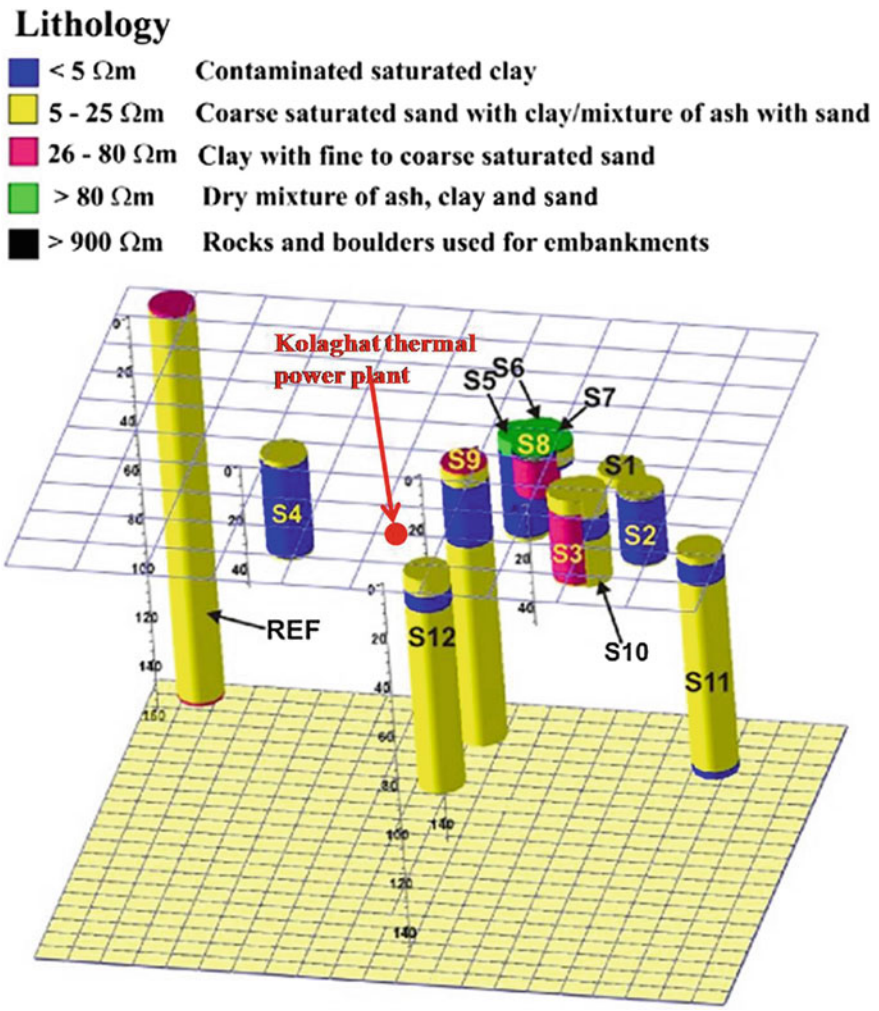



**Fig. 2** Geoelectric section from the vicinity of Kolaghat thermal power plant derived from interpreted resistivity and borehole log (modified after Parial et al. 2015)

As, Zn, Ag, Pb, Cr, Mn, Se, Cd, Cu) indicating the high concentration of various ionic species within the clay layer.

We analyzed the ash samples from three power stations located in West Bengal (Kolaghat, Durgapur, and Bandel). Tables 1, 2, and 3 show the results of radiometric analysis from these power stations (Mondal et al. 2006). Kolaghat ash showed the activity concentration variation of $^{232}$Th, $^{238}$U, and $^{40}$K in the range from 126 to 146 Bq kg$^{-1}$ (average 140 Bq kg$^{-1}$), 98–119 Bq kg$^{-1}$ (average 111 Bq kg$^{-1}$), and 266–415 Bq kg$^{-1}$ (average 351 Bq kg$^{-1}$), respectively. Similarly, the activity concentration variations of $^{232}$Th on

**Table 1** Radioactivity measurements in fly ash samples from Kolaghat thermal power station, West Bengal (after Mondal et al. 2006)

| Sample No. | $^{238}$U (Bq kg$^{-1}$) | $^{232}$Th (Bq kg$^{-1}$) | $^{40}$K (Bq kg$^{-1}$) | Dose rate (nGy h$^{-1}$) | Annual external effective dose rate (mSv y$^{-1}$) | $Ra_{eq}$ (Bq kg$^{-1}$) | $H_{ex}$ (Bq kg$^{-1}$) |
|---|---|---|---|---|---|---|---|
| KAP1 | 117.4 | 145.8 | 403.0 | 159.1 | 0.195 | 357 | 0.96 |
| KAP2 | 119.8 | 146.7 | 279.0 | 155.6 | 0.191 | 351 | 0.95 |
| KAP3 | 114.9 | 144.2 | 282.1 | 151.9 | 0.186 | 343 | 0.92 |
| KAP4 | 117.4 | 143.0 | 266.6 | 151.8 | 0.186 | 342 | 0.92 |
| KAP5 | 98.9 | 141.8 | 372.0 | 146.8 | 0.180 | 330 | 0.89 |
| KAP6 | 110.0 | 146.7 | 272.8 | 150.8 | 0.185 | 341 | 0.92 |
| KAP7 | 117.5 | 136.2 | 372.0 | 152.1 | 0.187 | 341 | 0.92 |
| KAP8 | 108.0 | 136.4 | 372.0 | 147.8 | 0.181 | 332 | 0.89 |
| KAP9 | 113.7 | 126.1 | 359.6 | 143.7 | 0.176 | 322 | 0.87 |
| KAP10 | 108.4 | 138.7 | 384.4 | 149.9 | 0.184 | 336 | 0.91 |
| KAP11 | 107.2 | 139.7 | 368.9 | 149.3 | 0.183 | 335 | 0.90 |
| KAP12 | 107.5 | 146.3 | 415.4 | 155.3 | 0.191 | 348 | 0.94 |
| KAP13 | 113.9 | 141.4 | 403.0 | 154.9 | 0.190 | 347 | 0.94 |
| KAP14 | 105.2 | 129.7 | 359.6 | 141.9 | 0.174 | 318 | 0.86 |
| Mean | 111.4 | 140.2 | 350.7 | 150.8 | 0.185 | 339 | 0.91 |

Durgapur and Bandel Thermal Power Stations indicate an average value of 107 and 106 Bq kg$^{-1}$ (ranged from 62 to 139 Bq kg$^{-1}$), respectively.

On comparing the variation in radionuclides activity concentration measured at these power stations, it indicated that the enrichment of a particular radionuclide in the ashes is different at different power stations. Here, Kolaghat ashes indicate maximum enrichment of $^{232}$Th compared to Durgapur and Bandel ashes. However, Bandel ashes are enriched in $^{238}$U. Durgapur ashes show lesser activity concentration for $^{40}$K compared to Kolaghat and Bandel ashes. Ashes from these power stations show more activity concentration for $^{232}$Th compared to $^{238}$U activity concentration. The feed coal analysis from these power plants also indicates the maximum activity concentration of $^{232}$Th compared to $^{238}$U (Mandal and Sengupta 2003). These power plants infer to the high radionuclides activity concentration compared to the power plants located in other parts of India. Table 4 shows the mean activity coefficients of radionuclides (U, Th, and K) and absorbed dose rates of fly ashes from other thermal power plants (Mondal et al. 2006).

Due to the presence of uranium in the organic material in sedimentary rocks, it accumulates in coal, during the formation of coal. Uranium is mainly retained in the carbonaceous part, due to sorptive uptake during the initial stages of peat accumulation and subsequent burial (Zielinski et al. 1986). In contrast, the inorganic phases retain most of the thorium. The geological formation around the ash ponds

**Table 2** Radioactivity measurements in fly ash of Durgapur thermal power plant (after Mondal et al. 2006). The annual external effective dose rate (mSv $y^{-1}$), radium equivalent activity ($Ra_{eq}$), and external hazard index ($H_{ex}$) have also been provided

| Sample No. | $^{238}U$ (Bq $kg^{-1}$) | $^{232}Th$ (Bq $kg^{-1}$) | $^{40}K$ (Bq $kg^{-1}$) | Dose rate (nGy $h^{-1}$) | Annual external effective dose rate (mSv $y^{-1}$) | $Ra_{eq}$ (Bq $kg^{-1}$) | $H_{ex}$ (Bq $kg^{-1}$) |
|---|---|---|---|---|---|---|---|
| DAP1 | 96.6 | 109.1 | 300.7 | 123.1 | 0.142 | 276 | 0.74 |
| DAP2 | 93.1 | 105.3 | 280.1 | 118.3 | 0.142 | 265 | 0.71 |
| DAP3 | 96.5 | 109.3 | 290.4 | 122.7 | 0.145 | 275 | 0.74 |
| DAP4 | 94.1 | 101.0 | 267.3 | 115.7 | 0.159 | 259 | 0.70 |
| DAP5 | 85.4 | 107.6 | 272.4 | 115.8 | 0.146 | 260 | 0.70 |
| DAP6 | 96.5 | 98.1 | 354.7 | 118.6 | 0.157 | 264 | 0.71 |
| DAP7 | 100.4 | 113.9 | 344.4 | 129.5 | 0.150 | 290 | 0.78 |
| DAP8 | 95.6 | 103.8 | 287.8 | 118.8 | 0.157 | 266 | 0.72 |
| DAP9 | 100.4 | 110.0 | 364.9 | 128.1 | 0.143 | 286 | 0.77 |
| DAP10 | 99.6 | 104.0 | 326.4 | 122.4 | 0.158 | 273 | 0.74 |
| DAP11 | 101.7 | 112.0 | 321.3 | 128.0 | 0.161 | 287 | 0.77 |
| DAP12 | 99.3 | 96.0 | 313.5 | 116.9 | 0.156 | 261 | 0.70 |
| DAP13 | 102.9 | 112.0 | 334.1 | 129.1 | 0.142 | 289 | 0.78 |
| DAP14 | 96.7 | 120.0 | 336.7 | 131.2 | 0.142 | 294 | 0.79 |
| DAP15 | 100.4 | 110.3 | 341.8 | 127.3 | 0.145 | 284 | 0.77 |
| Mean | 97.3 | 107.8 | 315.8 | 123.0 | 0.150 | 275 | 0.74 |

**Table 3** Radioactivity measurements on fly ash samples of Bandel thermal power plant (after Mondal et al. 2006). The Ra equivalent activity ($Ra_{eq}$) and external Hazard index ($H_{ex}$) are also provided

| Sample No. | $^{238}U$ (Bq $kg^{-1}$) | $^{232}Th$ (Bq $kg^{-1}$) | $^{40}K$ (Bq $kg^{-1}$) | Dose rate (nGy $h^{-1}$) | Annual external effective dose rate (mSv $y^{-1}$) | $Ra_{eq}$ (Bq $kg^{-1}$) | $H_{ex}$ (Bq $kg^{-1}$) |
|---|---|---|---|---|---|---|---|
| BAP1 | 116.7 | 139.9 | 327.7 | 152.0 | 0.186 | 342 | 0.92 |
| BAP2 | 128.4 | 123.9 | 296.9 | 146.6 | 0.180 | 328 | 0.89 |
| BAP3 | 133.4 | 111.6 | 332.8 | 142.9 | 0.175 | 319 | 0.86 |
| BAP4 | 78.5 | 62.8 | 307.2 | 87.0 | 0.107 | 192 | 0.52 |
| BAP5 | 183.4 | 118.2 | 174.1 | 163.4 | 0.200 | 366 | 0.99 |
| BAP6 | 130.2 | 94.8 | 417.3 | 134.8 | 0.165 | 298 | 0.80 |
| BAP7 | 118.3 | 92.6 | 396.8 | 127.1 | 0.156 | 281 | 0.76 |
| Mean | 126.9 | 106.3 | 321.8 | 136.3 | 0.167 | 304 | 0.82 |

**Table 4** Mean activity of uranium, thorium, and potassium concentration along with absorbed dose rates of fly ash samples from some thermal power plants in India

| Thermal power stations (India) | Activity (Bq $kg^{-1}$) | | | Absorbed dose rates (nGt $h^{-1}$) | Reference |
|---|---|---|---|---|---|
| | $^{226}Ra$ | $^{228}Ac$ | $^{40}K$ | | |
| Allahabad (Uttar Pradesh) | 78.4 | 89.1 | 362.7 | 107.59 | Vijayan and Behera (1999) |
| Angul (Odisha) | 78.5 | 86.5 | 278.1 | 102.38 | Vijayan and Behera (1999) |
| Badarpur (Delhi) | 75.5 | 88.1 | 286.4 | 102.50 | Vijayan and Behera (1999) |
| Chandrapur (Madhya Pradesh) | 58.2 | 89.2 | 301.2 | 96.46 | Vijayan and Behera (1999) |
| Raichur (Karnataka) | 83.1 | 102.5 | 334.1 | 117.27 | Vijayan and Behera (1999) |
| Talchir (Odisha) | 79.2 | 96.3 | 291.6 | 109.73 | Vijayan and Behera (1999) |
| Bokaro (Bihar) | 70.3 | 118.4 | 252.0 | 118.91 | Lalit et al. (1986) |
| Ramagundam (Andhra Pradesh) | 59.2 | 95.1 | 507.0 | 109.38 | Lalit et al. (1986) |
| Neyvelli (Tamil Nadu) | 64 | 126.9 | 370.0 | 126.76 | Lalit et al. (1986) |
| Amarkantak (Madhya Pradesh) | 49.2 | 106.2 | 329.3 | 105.04 | Lalit et al. (1986) |
| Nasik (Maharashtra) | 126.9 | 138.0 | 279.0 | 157.18 | Lalit et al. (1986) |
| Nellore (Andhra Pradesh) | 64 | 126.9 | 370.0 | 126.76 | Lalit et al. (1986) |
| Farakka (West Bengal) | 84.1 | 98.8 | 297.1 | 113.71 | Vijayan and Behera (1999) |
| Bakreshwar (West Bengal) | 76.3 | 87.5 | 288.1 | 102.52 | Vijayan and Behera (1999) |
| Kolaghat (West Bengal) | 111.4 | 140.2 | 350.7 | 150.8 | Mondal et al. (2006) |
| Durgapur (West Bengal) | 97.3 | 107.5 | 315.8 | 123.0 | Mondal et al. (2006) |
| Bandel (West Bengal) | 126.9 | 106.3 | 321.8 | 136.3 | Mondal et al. (2006) |

of these power plants is mainly laterites overlained by clay. Clays are considered as potential trace elemental repositories. Therefore, the mixture of dry ashes and clay forms the top soil around these three thermal power plants. This facilitates the adsorption of radionuclides on the top soil (clayey layer). Due to the volatile nature of uranium, it migrates deeper by the percolating rain water and subsurface run-off; however, thorium remains adsorbed on the clayey formations. This is the reason that the ash samples show high activity concentration for $^{232}Th$ compared to $^{238}U$. Hence, the dose rates of the measured ash samples are following the trend of thorium activity concentration, which mean high concentration thorium contributes more in the dose rate. The activity concentration of the natural radionuclides in feed coal samples is 2–3 times lesser than the ash samples (Fig. 3).

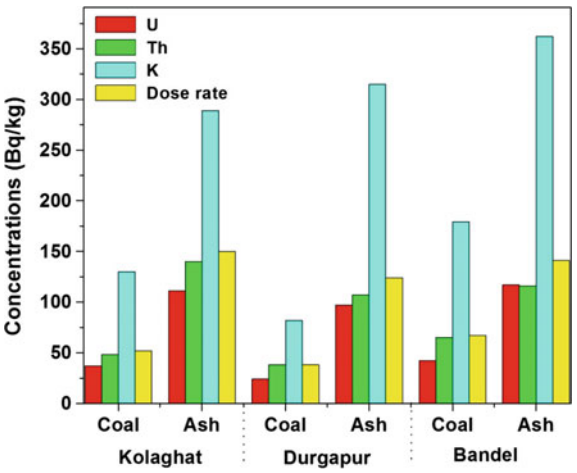



**Fig. 3** Radioactivity enhancement from coal to ash in Kolaghat, Durgapur, and Bandel thermal power plants (after Mondal et al. 2006)

To estimate the external gamma dose and internal dose due to radon and its daughters, $Ra_{eq}$ is calculated (Tables 1, 2, and 3) for the ash samples. The maximum permissible value for $Ra_{eq}$ is 370 Bq $kg^{-1}$ and for external hazard index ($H_{ex}$) is unity. These values are calculated using Eqs. (5) and (6).

In order to monitor the migration of contaminants laterally, several soil samples were collected and analyzed. High radioactivity was observed within a radius of 500 m and it decreases as we move further away from the ash ponds (Parial et al. 2016).

Nowadays, fly ash is being utilized in civil constructions in several forms; therefore, the radiation potential estimation becomes necessary (Eisenbud and Gesell 1997; MacKenzie 2000; UNSCEAR 1993, 2000). On comparison with coal, enhanced levels of uranium are present in fly ash (Jojo et al. 1993). Therefore, it is not easy to calculate the radon exhalation rate by uranium's or its daughter product's concentration due to its dependence on the texture and grain size composition (Tufail et al. 1991). Interestingly, the radon exhalation values are more in coal samples compared to fly ash samples. This may be due to the difference in the texture of coal and fly ash. In addition, the finer fly ash particles fill the small voids in the material and check the radon escape.

Easy availability and low cost of fly ash makes it an attractive substitute as building materials. In order to limit the radiation potential, it can be used as an additive in building materials. Several studies are reported which show the influence of fly ash as an additive on radiation level. However, different results are reported by different groups. Some authors reported a decreasing trend in radon exhalation in the mixture of concrete and fly ash additives (Stranden 1983; Maraziotis 1985). On the contrary, others have reported opposite trend when fly ash was used as an additive in cement (Siotis and Wrixon 1984). Some case studies reported no significant change in radon exhalation in cement and soil samples after mixing of fly ash in it (Ulbak et al. 1984; Karmadoost et al. 1988).

**Table 5** Radon exhalation rate in cement and soil with different proportions of fly ash (expressed in weight percent) added in the samples of equal total weight (Kumar et al. 2005)

| Sample | Fly ash additive (%) | Track density ($cm^{-2}$ $d^{-1}$) | Radon activity (Bq $m^{-3}$) | Radon exhalation rate (mBq $m^{-2}$ $h^{-1}$) | Expected values from an arithmetic mean |
|---|---|---|---|---|---|
| *1. Cement* | | | | | |
| AC0 | 0 | 26.8 ± 1.5 | 482 ± 26 | 173 ± 9 | – |
| AC1 | 10 | 49.9 ± 2.0 | 891 ± 36 | 320 ± 13 | 207 |
| AC2 | 20 | 65.9 ± 2.3 | 1176 ± 41 | 422 ± 15 | 241 |
| AC3 | 30 | 67.5 ± 2.3 | 1206 ± 42 | 433 ± 15 | 275 |
| AC4 | 40 | 69.2 ± 2.4 | 1235 ± 42 | 443 ± 16 | 310 |
| AC5 | 50 | 79.1 ± 2.5 | 1412 ± 45 | 507 ± 17 | 344 |
| *2. Soil* | | | | | |
| AS0 | 0 | 100.9 ± 2.8 | 1803 ± 51 | 648 ± 18 | – |
| AS1 | 10 | 91.3 ± 2.7 | 1630 ± 49 | 586 ± 18 | 634 |
| AS2 | 20 | 75.5 ± 2.5 | 1348 ± 44 | 484 ± 16 | 621 |
| AS3 | 30 | 72.24 ± 2.4 | 1290 ± 43 | 463 ± 15 | 608 |
| AS4 | 40 | 65.16 ± 2.3 | 1163 ± 41 | 418 ± 15 | 595 |
| AS5 | 50 | 60.3 ± 2.2 | 1076 ± 39 | 387 ± 14 | 582 |

To obtain a statistically reliable correlation on the application of fly ash as an additive, the '*t*-test' was used on the measurements obtained. The results for a homogeneous mixture of (i) cement and fly ash and (ii) soil and fly ash, in varying amounts, are summarized in Table 5. The samples with fly ash as additive in cement samples have shown a gradual increase, whereas a decrease is seen in soil samples, subsequent to the addition of fly ash. The experimental values for mixtures of ash and cement are higher than the values expected from the computations based on relative proportions of ash and cement, respectively. An opposite trend was observed for mixtures of ash and soil. This indicates that the values for the admixture increase, if the additive has higher exhalation rate than the base material and decrease if the value for additives is less (Kumar et al. 2005). This has been attributed to the emanating powers of different materials and also due to the difference in the grain size. The results obtained are significant, in terms of appropriate suppression of radon.

## Fly Ash Remediation and Utilization

Both India and China have the highest fly ash production per year. However, the amount utilized is about 38–45 % only. This is compared to about 65 % fly ash utilization in U.S.A. (Basu et al. 2009; other references cited there-in).

The use of fly ash as agricultural amendment, fly ash bricks, cement, and concrete and in pavements and highways is of considerable significance. In addition,

they are being used in production of glasses and glass-ceramics (Barbieri et al. 1999), as well as utilized to construct fills and embankments, grouts for pavements, structural fills, and retaining walls (Lamb 1974). More recently coal ashes have also been suggested as potential sources for rare earth extraction including yttrium (Kashiwakura et al. 2013; Seredin and Dai 2012).

The Organization for Economic Cooperation and Development (OECD) has classified the coal ash byproducts as Green List waste. Under Basel Convention it is not considered as a waste. The coal ash byproducts have not been utilized in many countries; however, they have been neglected like a waste material. Lack in the availability of appropriate cost-effective technologies prevents the optimum utilization of fly ash in India (Bhattacharjee and Kandpal 2002).

Geologically, various toxic elements and natural radionuclides are present in coal. Therefore, after burning the coal, the residues either gaseous emission or solid wastes (fly and bottom ash) or liquid discharge (leachates from ash ponds) are having these elements. According to Gabbard (1993), burning of the coal reduces the coal volume by 85 %, which mean that the radionuclides and trace elements are more concentrated in the residues (Technologically Enhanced Naturally Occurring Radioactive Material, TENORM). The partitioning behavior and fate are decided by combustion environment and the association of these elements with different phases/matrixes in coal (Papastefanou 2010; Karangelos et al. 2004). Due to the presence of $^{232}$Th in inorganic matrix and $^{238}$U in organic matrix, $^{238}$U and $^{232}$Th partition differently during combustion (Menon et al. 2011). $^{238}$U shows a preference for fine to ultrafine ash particles and are mostly released in the ambient environment through the stack (Papastefanou 2010; Coles et al. 1979). However, $^{232}$Th shows no preferential partitioning (Papastefanou 2010). The overall impact due to the radioactivity of the ash thus is mainly dependent on the type and amount of coal burnt for the energy generation. Therefore, the type and amount of coal burnt in the power production will be the deciding factor for radiation impact due to the radioactivity of the end products.

## Conclusions

The radioactivity analysis presented in this chapter shows considerable amount of contamination of the surface soil in the vicinity of the ash ponds. It has also been observed that the surface soil contamination is more prominent in the predominant wind direction. The background radioactivity, calculated from the emitted dose, of the ambient environments of Kolaghat, Durgapur, and Bandel thermal power plants is approximately three times higher than the world average of 43 nGyh$^{-1}$. The ashes from these power plants have 2–3 times more concentration of natural radionuclides than feed coal. Consequently, the populations living in the nearby areas are at higher health risk. The radium equivalent activity ($Ra_{eq}$) and external hazards index ($H_{ex}$) values are close to 370 Bq kg$^{-1}$ and unity, respectively. Therefore, the

amount of ash used as additives in building materials should be examined cautiously in order to keep a check on the concentration of natural radionuclides.

Among the leading available technologies for the remediation of heavy metal contaminated soils are immobilization, soil washing, and phytoremediation but have been frequently practiced in developed countries. These technologies are suggested for field applicability and commercialization in the developing countries, where environmental degradation is the rancorous legacy of the urbanization, industrialization, and agricultural activities.

## References

Abd El-mageed AI, El-Kamel AH, Abbady A, Harb S, Youssef AMM and Saleh II (2011) Assessment of natural and anthropogenic radioactivity levels in rocks and soils in the environments of Juban town in Yemen. Radiat Phys Chem 80:710–715

Barbieri L, Lancellotti I, Manfredini T, Queralt I, Rincon JM, Romero M (1999) Design, obtainment and properties of glasses and glass ceramics from coal fly ash. Fuel 78(2):271–276

Basu M, Pande M, Bhadoria PBS, Mahapatra SC (2009) Potential fly-ash utilization in agriculture: a global review. Prog Nat Sci 19:1173–1186

Bhattacharjee U, Kandpal TC (2002) Potential of flyash utilisation in India. Energy 27:151–166

Coles DG, Ragaini RC, Ondov JM, Fisher GL, Silberman D, Prentice BA (1979) Chemical studies of stack fly ash from a coalfired power plant. Environ Sci Technol

Culec N, Gunal (Calci) B, Erler A (2001) Assessment of soil and water contamination around an ash-disposal site: a case study from the Seyitomer coal-fired power plant in western Turkey. Environ Geol 40:331–344

Eisenbud M, Gesell T (1997) Environmental radioactivity, 4th edn. Academic Press, San Diego

Fleischer RL, Morgo-campero A (1978) Mapping and integrated radon emanation for detection of long distance migration of gases within the earth, techniques and principles. Geophys Res 83:3539–3549

Gabbard A (1993) Coal combustion—ORNL review. Oak Ridge Natl Lab Rev 26(3&4):24–33

Jojo PJ, Rawat A, Kumar A, Prasad R (1993) Trace uranium analysis in Indian coal samples. Nucl Geophys 7:445–448

Karangelos DJ, Petropoulos NP, Anagnostakis MJ, Hinis EP, Simopoulos SE (2004) Radiological characteristics and investigation of the radioactive equilibrium in the ashes produced in lignite-fired power plants. J Environ Radioact

Karmadoost NA, Durrani SA, Fremlin JH (1988) An investigation of radon exhalation from fly ash produced in the combustion of coal. Nucl Tracks Radiat Meas 15:647–650

Kashiwakura S, Kumagai Y, Kubo H, Wagatsuma K (2013) Dissolution of rare earth elements from coal fly ash particles in a dilute H2SO4 solvent, Open J Phys Chem 3:69–75

Khan K, Aslam M, Orfi SD, Khan HM (2002) Norm and associated radiation hazards in bricks fabricated in various localities of the North-West Frontier Province (Pakistan). J Environ Radioact 58:59–66

Khan AJ, Prasad R, Tyagi RK (1992) Measurement of radon exhalation rate from some building materials. Nucl Tracks Radiat Meas 20:609–610

Kumar R, Mahur AK, Sengupta D, Prasad R (2005) Radon activity and exhalation measurements in fly ash from a thermal power plant. Radiat Meas 40:638–641

Lalit BY, Ramachandran TV, Mishra UC (1986) Radiation exposures due to coal-fired power stations in India. Radiat Protect Dosimetry 15:197–202

Lamb DW (1974) Ash disposal in dams, mounds, structural fills and retaining walls. In: Proceedings of the third international ash utilization symposium. U.S. Bureau of Mines, Information Circular No. 8640, Washington DC

MacKenzie AB (2000) Environmental radioactivity: experience from the 20th century-trends and issues for the 21st century. Sci Total Environ 249:313–329

Maharana, M, Eappen KP, Sengupta D (2010) Radon emanometric technique for $^{226}$Ra estimation. J Radioanal Nucl Chem 285(3):469–474

Mandal A, Sengupta D, Sharma SP (2007) DC Resistivity studies for mapping groundwater contamination in and around ash-disposal site of Kolaghat thermal power plant, West Bengal. J Geol Soc India 69:373–380

Mandal A, Sengupta D (2006) An assessment of soil contamination around coal-based thermal power plant in India. Environ Geol 51(3):409–420

Mandal A, Sengupta D (2003) Radioelemental study of Kolaghat thermal power plant, West Bengal, India—Possible environmental hazards. Environ Geol 44:180–187

Maraziotis EA (1985) Gamma activity of the fly ash from a Greek power plant and properties of fly ash in cement. Health Phys 49:302–307

Menon R, Raja P, Malpe D, Subramaniyam KSV, Balaram V (2011) Radioelemental characterization of fly ash from Chandrapur Super thermal power station, Maharashtra, India. Curr Sci 100:1880–1883

Mondal T, Sengupta D, Mandal A (2006) Natural Radioactivity of ash and coal in major thermal power plants of West Bengal, India. Curr Sci 91:1387–1393

Papastefanou C (2010) Escaping radioactivity from coal-fired power plants (CPPs) due to coal burning and the associated hazards: a review. J Environ Radioact

Parial K (2016) Integrated study for risk and vulnerability assessment using geochemical, Geophysical and geospatial analysis around Kolaghat thermal power plant, Eastern India, PhD. thesis, Indian Institute of Technology Kharagpur, India

Parial K, Guin R, Agrahari S, Sengupta D (2016) Monitoring of Radionuclide migration around Kolaghat thermal power plant, West Bengal, India. J Radioanal Nucl Chem 307(1):533–539

Parial K, Biswas A, Agrahari S, Sharma SP, Sengupta D (2015) Identification of contaminated zones using direct current (DC) resistivity surveys in and around ash ponds near Kolaghat thermal power plant, West Bengal, India. Int J Geol Earth Sci 1(2)

Seredin VV, Dai S (2012) Coal deposits as potential alternative sources for lantanidesnd yttrium 94:67–93

Singh S, Ram LC, Masto RE, Verma SK (2011) A comparative evaluation of minerals and trace elements in the ashes from lignite, coal refuse, and biomass fired power plants. Int J Coal Geol 87:112–120

Singh AK, Jojo PJ, Khan AJ, Prasad R, Ramchandran TV (1997) Calibration of track detectors and measurement of radon exhalation rate from solid samples. Radiat Prot Environ 3:129–133

Siotis I, Wrixon AB (1984) Radiological consequences of the use of fly ash in building materials in Greece. Radiat Prot Dosim 7:101–105

Stranden E (1983) Assessment of radiological impact of using fly ash in cement. Health Phys 44:145–151

Telford WM, Geldart LP, Sheriff RE (1990) Applied geophysics, 2nd edn. Cambridge University Press

Tufail M, Mirza SM, Chughati MK, Ahmad N, Khan HA (1991) Preliminary measurements of exhalation rates and diffusion coefficients for radon in cements. Nucl Tracks Radiat Meas 19:427–428

Ulbak K, Jonnassen J, Backmark K (1984) Radon exhalation from samples of concrete with different porosities and fly ash additives. Radiat. Prot. Dosim. 7:45–51

UNSCEAR (1993) Sources and effects of ionizing radiation. United Nations scientific committee on the effect of atomic radiation, United Nations, New York

UNSCEAR (2000) Sources and effects of ionizing radiation. United Nations scientific committee on the effect of atomic radiation, United Nations, New York

Vijayan V, Behera SN (1999) Studies on natural radioactivity in coal ash. In: Mishra PC, Naik A (eds) Environmental management in coal mining and thermal power plants. Technoscience, Jaipur, pp 453–456

Zielinski RA, Budahn JR (1986) Radionuclides in coal and coal combustion waste products: characterization of coal and coal combustion products from a coal-fired power plant. USGS Open File Report, pp 98–342

http://www.springer.com/978-981-10-2409-2

Modelling Trends in Solid and Hazardous Waste Management

Sengupta, D.; Agrahari, S. (Eds.)
2017, XI, 171 p. 41 illus., Hardcover
ISBN: 978-981-10-2409-2